Free-Radical Polymerizations Associated with the Trommsdorff Effect Under Semibatch Reactor Conditions. III. Experimental Responses to Step Changes in Initiator Concentration

V. DUA, D. N. SARAF, and SANTOSH K. GUPTA*

Department of Chemical Engineering, Indian Institute of Technology, Kanpur-208 016, India

SYNOPSIS

The presence of the diffusion-limited gel or Trommsdorff effect in free-radical polymerizations poses a challenge for the modeling of these reactors. The available models cannot be applied to industrial reactors because of their inability to account for nonisothermal effects and semibatch operations. Recent models have overcome these limitations. These models have already been validated for step changes in temperature. The validity of these models under semibatch reactor conditions has been established in the present investigation. Experiments have been carried out at constant temperatures (50 and 70°C) and a step change in the initiator concentration from about 15.48 to 100 mol/m^3 has been effected during the course of polymerization. Experimental results on monomer conversions and average molecular weights have been found to be in reasonable agreement with model predictions. The present study establishes the applicability of these models for more general semibatch reactor operations, as well as the possibility of model-based optimal control of industrial reactors. © 1996 John Wiley & Sons, Inc.

INTRODUCTION

Nonisothermal and semibatch operations are quite common in industrial free-radical polymerization [e.g., poly(methyl methacrylate) (PMMA) and polystyrene (PS)] reactors. A fundamental understanding of the physicochemical phenomena is required to incorporate these effects in a model, especially of the gel or Trommsdorff effect,[1,2] where the reactions become diffusion-controlled and evaluation of the overall rate constants becomes difficult. Various attempts to model these effects have been reviewed by O'Driscoll,[3] Hamielec,[4] Mita and Horie,[5] and Achilias and Kiparissides.[6,7] The phenomenological model of Chiu et al.[8] incorporates diffusional limitations as an integral part of the termination and propagation reactions. The appearance of this model led to several studies[9-11] on the optimization and parametric sensitivity of PMMA reactors. This model was extended by Achilias and Kiparissides[6,7] using the diffusion theory of Vrentas and Duda[12] and the theory of excess chain-end mobility.[13] The theory of Ray et al.[14] (Part I of this series) extends this work so as to apply it to semibatch reactors and reactors operating under nonisothermal operations. These workers assumed that the initiator efficiency, f, remains constant as the monomer conversion increases. Seth[15] and Seth and Gupta[16] improved on the model of Ray et al. by allowing the value of f to decrease at high conversions. The new model is found to be less sensitive to minor variations in the values of the parameters. The robustness of this model is useful for developing optimal control strategies for reactors.

Recently, Faldi et al.[17,18] measured diffusion coefficients of large and small molecules in polymeric solutions which simulate conditions under which the gel and glass effects occur. They inferred that the diffusion coefficients of polymeric radicals and primary radicals decrease significantly during poly-

* To whom correspondence should be addressed.

Journal of Applied Polymer Science, Vol. 59, 749–758 (1996)
 CCC 0021-8995/96/040749-10

merization as the monomer concentration decreases. These decreases correlate well with the decrease of the termination rate constant, k_t, and the initiator efficiency, f, with increasing monomer conversions. This justifies the use of models (e.g., Refs. 6–8 and 14–16) attempting to relate k_t and f with the diffusion coefficients. In contrast, the experimental values of the diffusion coefficients of a monomer do not decrease as rapidly as does the rate of propagation, k_p. They claimed that the success of models correlating k_p with the diffusion coefficients of the monomer is purely fortuitous. They, unfortunately, have not suggested models for k_p, and one, therefore, continues to use semiempirical models for the gel and glass effects, even though they have been only partly substantiated by the fundamental studies of Faldi et al.

There have been several experimental studies[19–21] on the control of free-radical polymerization reactors, but all of them have been restricted to solution polymerizations. No such studies have been reported on bulk free-radical polymerizations, even though this is of importance from an industrial point of view. Moreover, no work has been reported on the optimal control of these reactors using analytical models. The models of Ray et al.[14] and Seth and Gupta[15,16] appear to be well suited for both optimization and model-based control applications. The model parameters have been obtained (for the sample system, PMMA with AIBN as initiator) using experimental data of Balke and Hamielec[22] taken under isothermal conditions. These data were obtained by carrying out bulk polymerizations in small ampules where heat and mass transfer effects, mixing, and vaporization are not important. The "tuned" models[14–16] need to be tested out under nonisothermal conditions, as well as under semibatch reactor conditions.

Since temperature and initiator concentration are the two important control variables in free-radical polymerization systems, the models should be tested for step changes in these. These idealized operations are sufficient for checking the validity of the models for more general situations. The validity of the model of Ray et al. has been tested by Srinivas et al.[23] (Part II of this series) for step changes in temperature. They studied polymerization of MMA with step decreases and increases in the temperature and showed that the time of appearance of the gel effect could be speeded up or postponed depending upon the conditions of the reaction mass at the time at which the temperature was changed. Their experimental data agreed reasonably well with model predictions, *without any further tuning of the parameters.* The change in temperature also affected the molecular weights of the polymer formed. Thus, temperature could, indeed, be used as a control variable for obtaining polymer having desired properties.

In the present study, the recent model[15,16] has been tested against experimental results obtained with step increases in the initiator concentration. Experiments have been carried out at two values of the initial initiator concentration, $[I]_0$ (15.48 mol/m^3 and a reasonably large value of 100 mol/m^3), at two different temperatures (50 and 70°C) in a 1-L, PC-interfaced, stainless-steel Parr reactor. Data have also been taken with the initiator concentration increased suddenly from about 15.48 to about 100 mol/m^3 at a constant temperature. These runs provide dynamic data on conversions and molecular weights because of step changes in the initiator concentration. The results are found to compare well with theoretical predictions,[14–16] thus establishing the applicability of the models to more general semibatch operations used industrially.

THE MODEL

The model of Ray et al.[14] assumed the initiator efficiency, f, to be constant with time, while k_p and k_t were modeled to account for their decrease at high monomer conversions. It was found that the results were very sensitive to small variations in the parameters, θ_t and θ_p, used by these workers. This sensitivity was removed by Seth and Gupta,[16] who incorporated an equation for f, using a modification of the model of Achilias and Kiparissides.[7] Table I gives the final equations[15,16] describing the gel and glass effects, which need to be used along with appropriate mass-balance and moment equations. This table also includes the best-fit correlations for θ_t, θ_p, and f, obtained by curve-fitting the isothermal data of Balke and Hamielec[22] taken in small ampules. Since these equations involve only *instantaneous* values of variables, they apply to any reactor, including semibatch reactors operating under nonisothermal conditions.

EXPERIMENTAL

The experimental setup used earlier by Srinivas et al.[23] is modified to include an initiator displacement assembly (shown by the dotted region in Fig. 1). The initiator (dissolved in monomer) is placed in the container, C, before the start of polymerization and is discharged into the reactor by displacement

Table I Gel- and Glass-Effect Equations (15) and (16)

$$\frac{1}{f} = \frac{1}{f_0}\left[1 + \theta_f(T)\,\frac{M}{V_l}\,\frac{1}{\exp[\xi_{I3}\{-\psi + \psi_{\text{ref}}\}]}\right] \quad \text{(a)}$$

$$\frac{1}{k_t} = \frac{1}{k_{t,0}} + \theta_t(T)\,\mu_n^2\,\frac{\lambda_0}{V_l}\,\frac{1}{\exp[-\psi + \psi_{\text{ref}}]} \quad \text{(b)}$$

$$\frac{1}{k_p} = \frac{1}{k_{p,0}} + \theta_p(T)\,\frac{\lambda_0}{V_l}\,\frac{1}{\exp[\xi_{I3}\{-\psi + \psi_{\text{ref}}\}]} \quad \text{(c)}$$

$$\psi = \frac{\gamma\left\{\dfrac{\rho_m\phi_m\hat{V}_m^*}{\xi_{13}} + \dfrac{\rho_s\phi_s\hat{V}_s^*}{\xi_{23}} + \rho_p\phi_p\hat{V}_p^*\right\}}{\rho_m\phi_m\hat{V}_m^*V_{fm} + \rho_s\phi_s\hat{V}_s^*V_{fs} + \rho_p\phi_p\hat{V}_p^*V_{fp}} \quad \text{(d)}$$

$$\psi_{\text{ref}} = \frac{\gamma}{V_{fp}} \quad \text{(e)}$$

$$\xi_{13} = \frac{\hat{V}_m^*\,(\text{MW}_m)}{\hat{V}_p^*\,M_{jp}} \quad \text{(f)}$$

$$\xi_{23} = \frac{\hat{V}_s^*\,(\text{MW}_s)}{\hat{V}_p^*\,M_{jp}} \quad \text{(g)}$$

$$\xi_{I3} = \frac{\hat{V}_I^*\,(\text{MW}_I)}{\hat{V}_p^*\,M_{jp}} \quad \text{(h)}$$

$$k_d = k_d^0 \exp(-E_d/RT) \quad \text{(i)}$$

$$k_{p,0} = k_{p,0}^0 \exp(-E_p/RT) \quad \text{(j)}$$

$$k_{t,0} = k_{td,0} = k_{td,0}^0 \exp(-E_{td}/RT) \quad \text{(k)}$$

Best-fit correlation (BFCs) for the MMA–AIBN system:

$$\log_{10}[\theta_t(T), \text{s}] = 1.241 \times 10^2 - 1.0314 \times 10^5\,(1/T) + 2.2735 \times 10^7\,(1/T^2) \quad \text{(l)}$$

$$\log_{10}[\theta_p(T), \text{s}] = 8.03 \times 10^1 - 7.50 \times 10^4\,(1/T) + 1.765 \times 10^7\,(1/T^2) \quad \text{(m)}$$

$$\log_{10}[10^3\theta_f(T), \text{m}^3\ \text{mol}^{-1}] = 2.016 \times 10^2 - 1.455 \times 10^5\,(1/T) + 2.70 \times 10^7\,(1/T^2) \quad \text{(n)}$$

Other details provided in Refs. 14–16.

with argon to provide a step change in initiator concentration at the desired time. The exact sequence of operations performed for intermediate addition (IA) of the initiator to the reaction mass are given below:

1. Degassification of the displacement assembly is done through valve V_4, keeping V_2 and V_7 closed and V_4, V_5, and V_6 open. V_4 is then closed.
2. Argon is introduced with V_5 and V_6 open and V_2 and V_7 closed. The argon pressure is maintained at about the same value as that in the reactor (~960 kPa).
3. A Teflon plug is installed to prevent the leakage of argon.

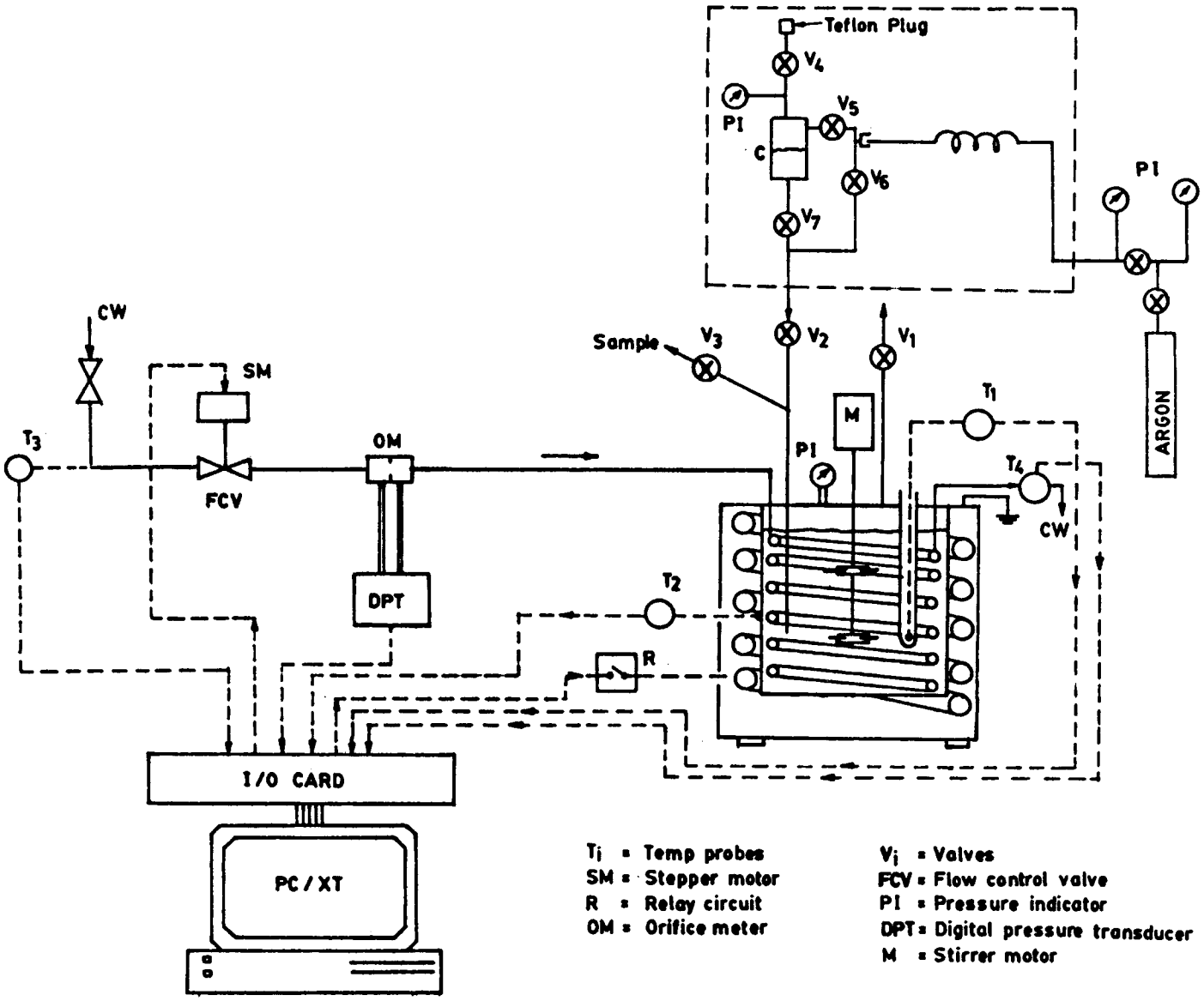

Figure 1 Schematic diagram of experimental setup. Dotted region indicates modifications made to the setup of Srinivas et al.[23]

4. During the time when no initiator is being transferred to the reactor and polymerization is taking place in the reactor, V_4, V_5, and V_7 are closed and V_6 and V_2 are open.
5. During IA, V_6 is closed and the initiator solution in C is pressurized to a pressure of about 55 kPa (as indicated by the pressure indicator atop the displacement assembly) above the value in the reactor.
6. V_7 is then opened to facilitate the flow of the initiator solution into the reactor. A whistling sound of the flowing solution is heard for about 5 s. One waits for about 60 s to ensure that the flow is complete.
7. V_7 is then closed and V_6 opened, simultaneously increasing the pressure by about 3.5 kPa to ensure transfer of the material which might have entered the tube between V_7 and V_6 into the reactor.
8. The displacement assembly is carefully washed with benzene soon after completion of the polymerization to avoid blockage of the valves due to the polymerization of residual monomer in it.

For the IA runs, the solution of initiator in the monomer is prepared about 30 min before the addition. This solution, 75 mL, is transferred from

Table II Details of Experimental Runs

Sample No.	Run No.	Initiator Concentration at $t = 0$ (mol/m^3)	IA Time t_{IA} (min)	Initiator Concentration After IA[a] (mol/m^3)	Experimental Temperature History[b] T (°C)
1	NI50c	15.48	—	—	$23.3777 - 0.04511740t + 0.37778t^2$; $t < 8.81$ 50; $t \geq 8.81$
2	NI50d	15.48	—	—	$31.747 - 0.000960385t + 0.370478t^2$; $t < 7.35$ 50; $t \geq 7.35$
3	NI50e	100.0	—	—	$36.0079 - 0.403046t + 0.408415t^2$; $t < 6.83$ 50; $t \geq 6.83$
4	NI50f	100.0	—	—	$27.5695 + 0.261781t + 0.363671t^2$; $t < 7.87$ 50; $t \geq 7.87$
5	NI70d	100.0	—	—	$35.188 + 2.65369t + 0.0362537t^2$; $t < 10.97$ 70; $t \geq 10.97$
6	NI70e	15.48	—	—	$35.288 + 1.41489t + 0.22145t^2$; $t < 9.96$ 70; $t \geq 9.96$
7	IA50a1	15.48	170	100.0	$25.2418 - 0.425326t + 0.414076t^2$; $t < 8.46$ 50; $t \geq 8.46$
8	IA50a2	15.48	170	100.0	$21.4078 + 0.424793t + 0.329944t^2$; $t < 9.16$ 50; $t \geq 9.16$
9	IA50b	15.48	90	100.0	$20.8212 - 0.10132t + 0.370111t^2$; $t < 9.13$ 50; $t \geq 9.13$
10	IA70a1	15.48	28	100.0	$22.7676 + 2.8778t + 0.0846003t^2$; $t < 12.65$ 70; $t \geq 12.65$
11	IA70a2	15.48	28	100.0	$20.8766 + 1.19t + 0.246t^2$; $t < 12.45$ 70; $t \geq 12.45$

[a] These are values that would have been obtained at $t = 0$ if the initiator–monomer solution was added at $t = 0$ itself to the reaction mass.

[b] t in min.

storage (in C) to the reactor in each IA run. The concentration of the initiator in this stored solution is such that *if this solution had been added to the reactor at time $t = 0$ the initiator concentration would have been* 100 mol/m^3. In this article, for the sake of brevity, whenever it is mentioned that IA leads to an increase in the initiator concentration from 15.48 to 100 mol/m^3, it is the *initial* values of the concentrations that we are really referring to, as described above.

The temperature-control system used in the present study is the same as that described by Srinivas et al.[23] with some minor modifications. A tape heater is wrapped on the argon line so as to increase its temperature to reasonable levels above the ambient. This avoids a temperature shock every time argon is introduced into the reactor, particularly during winter when the ambient temperature is less than about 10°C. During winter, the initial heating period (from room temperature to 50 or 70°C) increases to about 20 min. To reduce this period to more reasonable values of about 10 min, the reactor with monomer alone in it is first preheated to about 35°C. At this point, initiator (again dissolved in appropriate amounts of monomer so that the initiator concentration is $[I]_0$ after addition) is introduced from the initiator displacement assembly into the reactor. This is defined as $t = 0$. For IA runs during winter, a second transfer of initiator (in monomer) is effected during the course of polymerization, from the initiator displacement assembly. The controller parameters are also slightly readjusted during winter to keep the temperature within ±0.5°C. All other details of the experimental procedures followed, including purification of the reagents and analysis of the product, are identical to those used by Srinivas et al.[23]

RESULTS AND DISCUSSION

Bulk polymerizations were carried out at two different temperatures (50 and 70°C) and at two initiator loadings ($[I]_0 = 15.48$ and 100 mol/m^3). Table II gives details of the various experimental runs carried out in the present investigation. No interme-

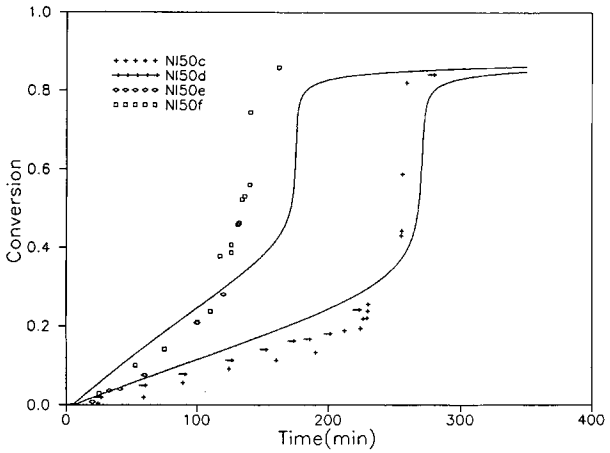

Figure 2 Conversion histories for MMA polymerization with AIBN for near-isothermal (NI50) runs ($T \sim 50°C$) in absence of IA of the initiator. Details as given in Table II. Theoretical predictions[15,16] on conversion, using the measured temperature histories (Table II) are shown by solid curves.

diate addition (IA) of initiator is done in the first six runs, whereas in the last five runs, IA leads to an instantaneous (step) increase in the initiator concentration during polymerization (from 15.48 to 100 mol/m^3, as per the nomenclature described earlier). Runs at serial numbers 2, 4, 8, and 11 were repeats of those at 1, 3, 7, and 10. These were done to check the reproducibility of the results. As discussed by Srinivas et al.,[23] the polymerization was carried out under near-isothermal (NI) conditions. There was an initial heating period when the temperature changed from ambient to the desired value of 50 or 70°C, followed by a period of constant temperature. The transient was fitted with a polynomial in a least-squares sense. The fitted equation for each run is also given in Table II.

Figure 2 shows conversion vs. time for the NI 50c, d, e, and f runs at 50°C (no IA). The first two runs correspond to an initial initiator concentration of 15.48 mol/m^3, whereas the last two are with $[I]_0$ = 100 mol/m^3. The solid curves are the predicted values using the model of Seth and Gupta.[16] Theoretical results using the model of Ray et al.[14] (with a different set of values of θ_t and θ_p than given in Table I) lie very close to those shown in Figure 2 (as well as in later plots) and are therefore not shown. As seen from the figure, the reproducibility of the data is good. The agreement with model predictions is also satisfactory. It may be noted that these model predictions are based on best-fit correlations (BFCs) given in Table I and obtained from experimental data of Balke and Hamielec[22] under isothermal conditions in ampules, and no further tuning has been resorted to. The initial initiator concentrations, $[I]_0$, studied by Balke and Hamielec range only from 15.48 to 25.8 mol/m^3. Considering this, the mismatch in Figure 2 for $[I]_0$ = 100 mol/m^3 is not too much. Figure 3 shows experimental molecular weights as a function of monomer conversion, x, for runs NI50c and NI50f. The two curves represent the weight-average molecular weights, M_w, predicted from the theoretical model.[15,16] The experimental molecular weights are obtained using intrinsic viscosity measurements as in our previous study.[23] The agreement between theory and experimental data is reasonable, considering the fact that the molecular weights from intrinsic viscosity measurements are lower than M_w and that the theoretical M_w from this family[6-8,14-16,24] of models (using a single k_t to estimate rate, M_n, and M_w) cannot be too good.[14,23] Figure 4 shows conversion vs. time for the NI70d and e runs at 70°C for $[I]_0$ of 100 and 15.48 mol/m^3, respectively. Figure 5 shows the corresponding molecular weights vs. conversion. The match with the theoretical predictions[15,16] is found to be better than at 50°C.

It must be noted that the model predictions in Figures 2–5 are made using parameters as determined from data[22] in which $[I]_0$ was in the range of 15.48 to 25.8 mol/m^3. The fact that the same parameters are used to make predictions at a very high initiator loading of 100 mol/m^3, and the reasonable

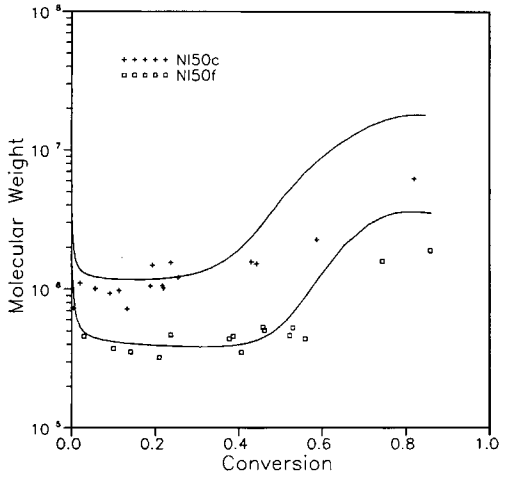

Figure 3 Molecular-weight histories for MMA polymerization with AIBN for near-isothermal (NI50) runs ($T \sim 50°C$) in absence of IA of the initiator. Details as given in Table II. Experimental data are from intrinsic viscosity measurements. Theoretical predictions[15,16] on M_w using the measured temperature histories (Table II) are shown by solid curves.

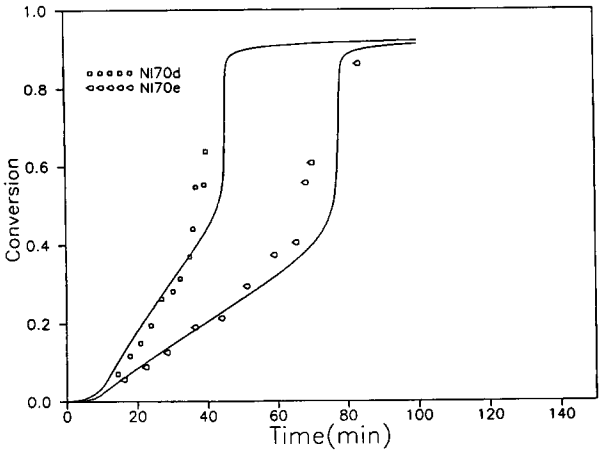

Figure 4 Conversion histories for MMA polymerization with AIBN for near-isothermal (NI70) runs ($T \sim 70°C$) in absence of IA of the initiator. Details as given in Table II and Figure 2.

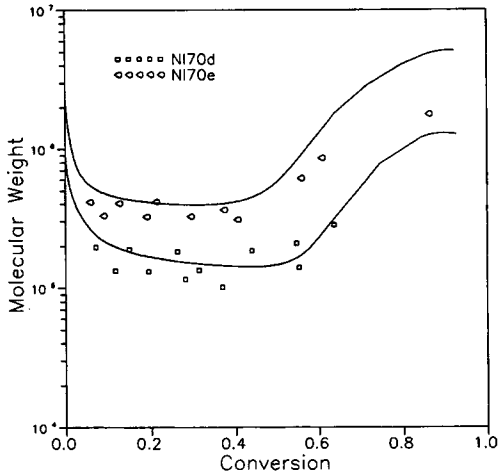

Figure 5 Molecular-weight histories for MMA polymerization with AIBN for near-isothermal (NI70) runs ($T \sim 70°C$) in absence of IA of the initiator. Details as given in Table II and Figure 3.

match with experimental data observed under these conditions, shows the generality of the model and its ability to predict far beyond the admissible range of $[I]_0$.

In the semibatch (IA) experiments, the initial initiator concentration of 15.48 mol/m^3 was increased to 100 mol/m^3 (as per the nomenclature defined in Table II) at some time, t_{IA}, by introducing additional initiator (and monomer) in a steplike manner. The time, t_{IA}, at which the intermediate solution was added was so adjusted that the gel-effect region became distinctly shifted away from the curves in Figure 2, for the case where there was no IA of the initiator solution. Keeping in view the experimental uncertainty, it was decided to choose two different values of t_{IA} for the 50°C runs. To make rough estimates of the t_{IA}, trial runs were made in small test tubes in a constant temperature bath where the appearance of the gel-effect region was ascertained visually. At 70°C, however, only one IA run was performed because of the narrow time gap between the gel-effect regions for the $[I]_0$ = 15.48 and 100 mol/m^3 runs.

Figure 6 shows experimental conversion data for the duplicate runs, IA50a1 and IA50a2, for IA at 170 min after the start of polymerization, along with the theoretically predicted curve. The curves on either side of this represent the theoretical conversions for 100 and 15.48 mol/m^3 initiator loadings. The IA curve follows the $[I]_0$ = 15.48 mol/m^3 curve until 170 min, and then a small dip is observed in the monomer conversion. This is because of the fact that along with the initiator some amount of unreacted monomer (used to dissolve the initiator) also enters the reactor, thus lowering the overall conversion (based on total monomer added). However, because of high initiator concentrations after the IA, the gel-effect sets in quickly and the conversion rises sharply. The experimental results follow model predictions quite closely. Figure 7 shows corresponding molecular weights as a function of conversion. The experimental points in the gel-effect region for the IA case lie in between the experimental points for the constant $[I]_0$ cases, as predicted theoretically,[15,16] even though quantitative agreement in the gel region is not as good. Again, the predictions from the model

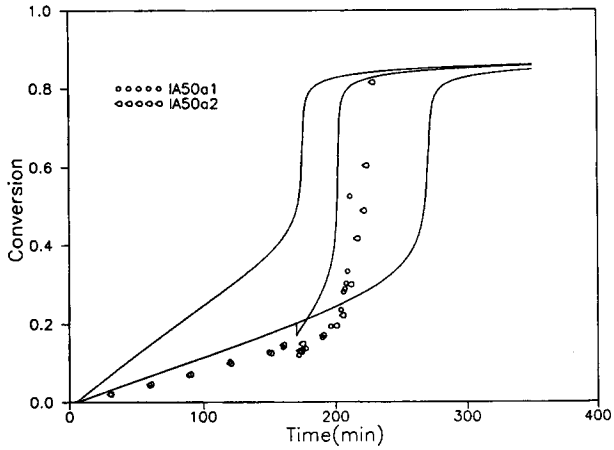

Figure 6 Conversion histories for MMA polymerization with AIBN for the IA50a1 and a2 ($T \sim 50°C$) runs (see Table II for details). Theoretical predictions[15,16] using the measured temperature histories (Table II) shown by the middle curve. Theoretical curves for the NI50c and NI50f cases (as in Fig. 2) shown for comparison.

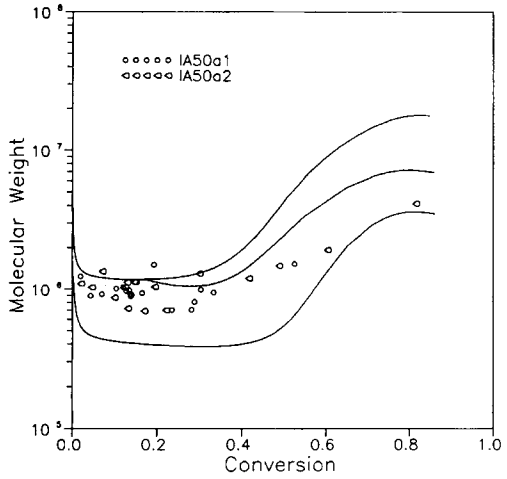

Figure 7 Molecular-weight histories for MMA polymerization with AIBN for the IA50a1 and a2 ($T \sim 50°C$) runs (see Table II and Fig. 3 for details). Theoretical predictions[15,16] of M_w using the measured temperature histories (Table II) shown by the middle curve. Theoretical curves for M_w for the NI50c and NI50f cases (as in Fig. 3) shown for comparison.

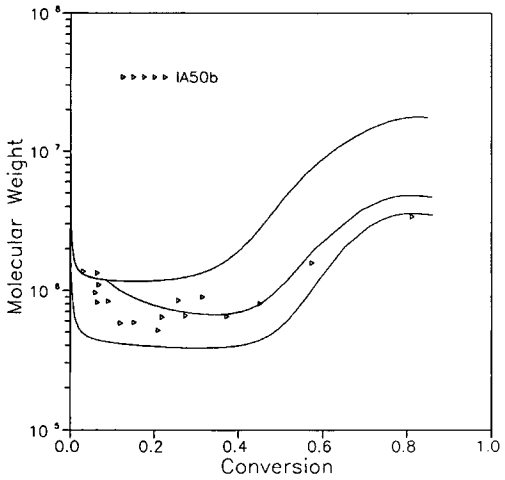

Figure 9 Molecular-weight histories for MMA polymerization with AIBN for the IA50b ($T \sim 50°C$) runs (see Table II and Fig. 3 for details). Theoretical predictions[15,16] of M_w using the measured temperature histories (Table II) shown by the middle curve. Theoretical curves for M_w for the NI50c and NI50f cases (as in Fig. 3) shown for comparison.

of Ray et al.[14] are very close to those from Seth and Gupta[16] and are not shown. Another IA run (IA50b) was carried out under the same conditions, except that t_{IA} was 90 min instead of 170 min. Figures 8 and 9 show the results on conversion and molecular weight. The inferences are similar to those made from Figures 6 and 7.

To further validate the model, we decided to repeat the IA runs at 70°C. This was done to check the strength of the model under varied conditions. Duplicate IA runs (IA70a1 and IA70a2; Figs. 10 and 11) were carried out at 70°C. The value of t_{IA} was 28 min. Reproducibility of the experimental data is observed to be quite good. The agreement of data with model predictions is again observed to be good.

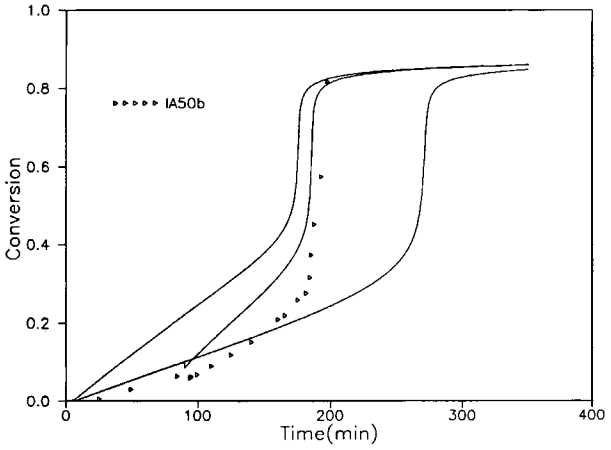

Figure 8 Conversion histories for MMA polymerization with AIBN for the IA50b ($T \sim 50°C$) runs (see Table II for details). Theoretical predictions[15,16] using the measured temperature histories (Table II) shown by the middle curve. Theoretical curves for the NI50c and NI50f cases (as in Fig. 2) shown for comparison.

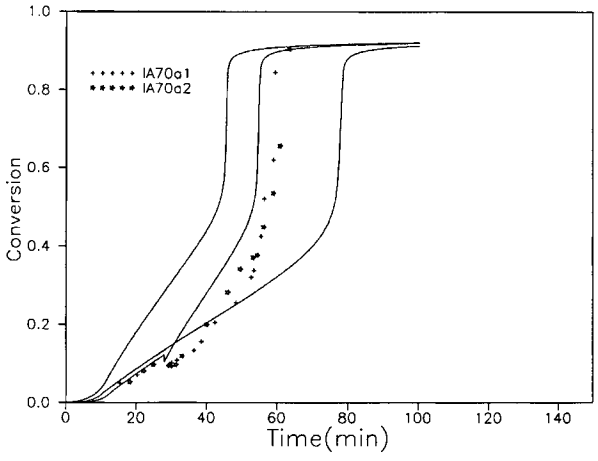

Figure 10 Conversion histories for MMA polymerization with AIBN for the IA70a1 and a2 ($T \sim 70°C$) runs (see Table II for details). Theoretical predictions[15,16] using the measured temperature histories (Table II) shown by the middle curve. Theoretical curves for the NI70d and NI70e cases (as in Fig. 4) shown for comparison. The slight difference in the theoretical plots in the early stages is due to slightly different temperature histories for the two runs.

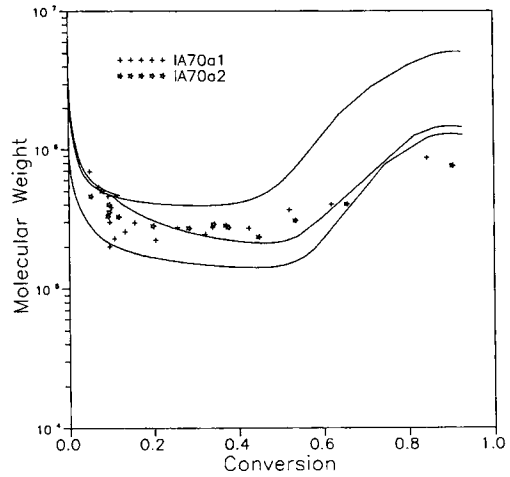

Figure 11 Molecular-weight histories for MMA polymerization with AIBN for the IA70a1 and a2 ($T \sim 70°C$) runs (see Table II and Fig. 5 for details). Theoretical predictions[15,16] of M_w using the measured temperature histories (Table II) shown by the middle curve. Theoretical curves for the NI70d and NI70e cases (as in Fig. 5) shown for comparison.

It may be added that we could further improve the agreement between experimental data and model predictions[15,16] by retuning the values of the parameters on the data reported herein. This could *possibly* be of use for on-line optimizing control studies. However, the agreement of present data on step-change experiments with model results (without retuning of parameters) is considered to be satisfactory enough to justify the use of the model for *more general* manipulations in the initiator concentration. Together with similar conclusions drawn by our earlier study[23] on the good agreement between experimental data and model results for step changes in temperature, we can state with some degree of confidence that the theoretical model of Seth and Gupta[16] (or of Ray et al.,[14] which does not give results which are too different) is now validated for the study of more general operating conditions in industrial semibatch reactors operating nonisothermally.

CONCLUSIONS

An experimental arrangement has been made to charge monomer, initiator, etc., to a 1-L well-mixed reactor during the course of polymerization. Data have been generated for constant initiator loadings, as well as for intermediate addition of an initiator. The agreement between experimental results and model predictions is quite good, considering the fact that the model parameters have been estimated from isothermal data on small ampules taken over a restricted range of $[I]_0$ values, and no retuning of these has been done. With the model now validated for step changes in both temperature[23] and initiator concentration (this work), we can use it for simulating semibatch PMMA reactors, operating nonisothermally. The model can also be used for implementing on-line optimizing control on these reactors. The model is quite general and can be used for other polymerization systems (e.g., PS and PVAc) as well, provided that model parameters are available for these systems.

This work was supported, in part, through financial support received from the Council of Scientific and Industrial Research, New Delhi, India, through Scheme No. 22(0232)/93/EMR-II.

NOMENCLATURE

E_d, E_p, E_t	activation energies for initiation, propagation, and termination in absence of gel or glass effects (kJ mol^{-1})
f	initiator efficiency at time t
f_0	initiator eficiency in the limiting case of zero diffusional resistance
I	initiator
IA	intermediate addition (of initiator–monomer solution)
$[I]_0$	initial concentration of initiator (initiator loading) (mol m^{-3})
k_d, k_p, k_t	rate constants for initiation, propagation, and termination in presence of the gel and glass effects (s^{-1} or m^3 mol^{-1} s^{-1})
k_d^0, $k_{p,0}^0$, $k_{t,0}^0$	frequency factors for initiation, propagation, and termination in absence of the gel and glass effects (s^{-1} or m^3 mol^{-1} s^{-1})
$k_{t,0}$, $k_{p,0}$	k_t and k_p in absence of gel and glass effects (m^3 mol^{-1} s^{-1})
M	moles of monomer in liquid phase (mol)
M_{jp}	molecular weight of polymer jumping unit (kg mol^{-1})
M_n	number-average molecular weight (g mol^{-1})

M_w	weight-average molecular weight (g mol^{-1})
(MW_I), (MW_m), (MW_s)	molecular weights of pure initiator, monomer, and solvent (kg mol^{-1})
R	universal gas constant (kJ mol^{-1} K^{-1})
S	solvent (none in this study)
t	time (s or min)
t_{IA}	time at which (instantaneous) intermediate addition of initiator–monomer solution is made (s or min)
T	temperature of reaction mixture at time t (K)
V_l	volume of liquid at time t (m^3)
V_{fm}, V_{fp}, V_{fs}	fractional free volumes of monomer, polymer, and solvent in reaction mixture
$\hat{V}_I^*$, $\hat{V}_m^*$, $\hat{V}_p^*$, $\hat{V}_s^*$	specific critical hole free volumes of initiator, monomer, polymer, and solvent (m^3 kg^{-1})
x	monomer conversion (molar)

Greek Letters

γ	overlap factor
θ_f, θ_p, θ_t	adjustable parameters in the model (m^3 mol^{-1}, s, and s, respectively)
λ_k	kth (k = 0, 1, 2, $\cdots$) moment of live (P_n) polymer radicals $\equiv \sum_{n=1}^{\infty} n^k P_n$ (mol)
μ_k	kth (k = 0, 1, 2, $\cdots$) moment of dead (D_n) polymer chains $\equiv \sum_{n=1}^{\infty} n^k D_n$ (mol)
μ_n	number-average chain length at time $t \equiv (\lambda_1 + \mu_1)/(\lambda_0 + \mu_0)$
ξ_{13}, ξ_{23}, ξ_{I3}	ratio of the molar volume of the monomer, solvent, and initiator jumping units to the critical molar volume of the polymer, respectively
ρ_m, ρ_p, ρ_s	density of pure (liquid) monomer, polymer or solvent at temperature T (at time t) (kg m^{-3})
ϕ_m, ϕ_p, ϕ_s	volume fractions of monomer, polymer, or solvent in liquid at time t
ψ, ψ_{ref}	defined in Table I, Eqs. (d) and (e)

REFERENCES

1. E. Trommsdorff, H. Köhle, and P. Lagally, *Makromol. Chem.*, **1**, 169 (1947).
2. R. G. W. Norrish and R. R. Smith, *Nature*, **150**, 336 (1942).
3. K. F. O'Driscoll, *Pure Appl. Chem.*, **53**, 617 (1981).
4. A. H. Hamielec, *Chem. Eng. Commun.*, **24**, 1 (1983).
5. I. Mita and K. Horie, *J. Macromol. Sci. Rev. Macromol. Chem. Phys.*, **C27**, 91 (1987).
6. D. Achilias and C. Kiparissides, *J. Appl. Polym. Sci.*, **35**, 1303 (1988).
7. D. S. Achilias and C. Kiparissides, *Macromolecules*, **25**, 3739 (1992).
8. W. Y. Chiu, G. M. Carratt, and D. S. Soong, *Macromolecules*, **16**, 348 (1983).
9. B. Kapoor, S. K. Gupta, and A. Varma, *Polym. Eng. Sci.*, **29**, 1246 (1989).
10. N. R. Vaid and S. K. Gupta, *Polym. Eng. Sci.*, **31**, 1708 (1991).
11. B. M. Louie and D. S. Soong, *J. Appl. Polym. Sci.*, **30**, 3707 (1985).
12. J. S. Vrentas and J. L. Duda, *AIChE J.*, **25**, 1 (1979).
13. S. K. Soh and D. C. Sundberg, *J. Polym. Sci. Polym. Chem. Ed.*, **20**, 1315 (1982).
14. A. B. Ray, D. N. Saraf, and S. K. Gupta, *Polym. Eng. Sci.*, **35**, 1290 (1995).
15. V. Seth, M. Tech. Dissertation, Indian Institute of Technology, Kanpur, 1995.
16. V. Seth and S. K. Gupta, *J. Polym. Eng.*, to appear.
17. A. Faldi, M. Tirrell, and T. P. Lodge, *Macromolecules*, **27**, 4176 (1994).
18. A. Faldi, M. Tirrell, T. P. Lodge, and E. von Meerwall, *Macromolecules*, **27**, 4184 (1994).
19. M. Soroush and C. Kravaris, *AIChE J.*, **38**, 1429 (1992).
20. M. F. Ellis, T. W. Taylor, and K. F. Jensen, *AIChE J.*, **40**, 445 (1994).
21. T. Peterson, E. Hernandez, Y. Arkun, and F. J. Schork, *Chem. Eng. Sci.*, **47**, 737 (1992).
22. S. T. Balke and A. E. Hamielec, *J. Appl. Polym. Sci.*, **17**, 905 (1973).
23. T. Srinivas, S. Sivakumar, S. K. Gupta, and D. N. Saraf, *Polym. Eng. Sci.*, to appear.
24. B. Agarwal and S. K. Gupta, *J. Polym. Eng.*, **12**, 257 (1993).

Received June 15, 1995
Accepted July 9, 1995